

## On the unsteady behavior of turbulence models

R. Rubinstein<sup>1</sup> and W.J.T. Bos<sup>2</sup>

<sup>1</sup>Newport News, Virginia, USA

<sup>2</sup>Université de Lyon - LMFA - CNRS UMR 5509 - Ecole Centrale de Lyon - UCBL - INSA Lyon, Ecully, France

Periodically forced turbulence is used as a test-case to evaluate the predictions of two-equation and multiple-scale turbulence models in unsteady flows. The limitations of the two-equation model are shown to originate in the basic assumption of spectral equilibrium. A multiple-scale model based on a picture of stepwise energy cascade overcomes some of these limitations, but the absence of nonlocal interactions proves to lead to poor predictions of the time variation of the dissipation rate. A new multiple-scale model that includes nonlocal interactions is proposed and shown to reproduce the main features of the frequency response correctly.

A basic premise of one point closures such as the  $k - \epsilon$  model is the hypothesis of "spectral equilibrium," which justifies two distinct roles of the dissipation rate  $\epsilon$ : on the one hand, it appears in the energy balance, defined as a correlation of velocity gradients, hence a small-scale quantity; on the other hand, it is used phenomenologically to describe large-scale transport properties. The most basic formulation of the latter is Kolmogorov's hypothesis  $\epsilon \propto k^{3/2}/L$  where  $k$  is the turbulent kinetic energy and where  $L$  is a length scale characteristic of the largest scales of motion; equivalent formulations include  $\nu_t \propto k^2/\epsilon$ , the formula for turbulent viscosity, or  $\tau \propto k/\epsilon$ , the formula for the turbulent time-scale. The Kolmogorov theory, or more general assumptions of self-similarity of all scales of motion, justify all of these proportionalities [1], although the constants of proportionality need not coincide in all self-similar flows [2].

But turbulence models are not needed to describe self-similar flows, which merely serve as calibration cases; models are needed to describe departure from self-similarity, when spectral equilibrium becomes a strong constraint on turbulence evolution. In a study of a flow in which turbulence evolves from a steady state to a self-similar time-dependent state [3], the implications of the departure from spectral equilibrium were investigated: this departure was connected to transient failure of the Tennekes-Lumley balance [4] and to the consequent relevance of small scale dynamics for the large scales. The breakdown of spectral equilibrium has also been observed in engineering flows including turbulent diffusers and wakes.[5]

The limitations of the spectral equilibrium hypothesis are very well known in the modeling literature and have led to proposals for *multiple-scale models* [6] that more realistically address the complexity of the non-linear interactions in turbulent flows. This letter reports on some investigations of multiple-scale models applied to an especially simple and attractive test case for transient turbulence: *periodically forced turbulence* [7–9]. This problem arises when isotropic incompressible turbulence, maintained in a steady state by a large-scale isotropic forcing with total amplitude  $\bar{p}$ , is subjected to a small time-dependent periodic perturbation with amplitude  $\tilde{p}$ :  $p(t) = \bar{p} + \tilde{p} \cos(\omega t)$ , such that the ratio

$\tilde{p}/\bar{p} \ll 1$  and such that the forcing length scale does not depend on time. The phase-averaged kinetic energy  $k$  can then be decomposed into a mean  $\bar{k}$  and a periodic part  $\tilde{k}(\omega) \cos(\omega t + \phi_k(\omega))$ , with  $\phi_k$  the phase-shift between the forcing and the kinetic energy. Similarly, the viscous dissipation rate can be written as  $\epsilon = \bar{\epsilon} + \tilde{\epsilon}(\omega) \cos(\omega t + \phi_\epsilon(\omega))$ ;  $\bar{k}$  and  $\bar{\epsilon}$  are related to the time-independent forcing length scale  $\bar{L}$  by  $\bar{L} \propto \bar{k}^{3/2}/\bar{\epsilon}$ . The periodic parts of  $k$  and  $\epsilon$  are sinusoidal, like the forcing, because  $\tilde{p}/\bar{p} \ll 1$ . The functions  $\tilde{k}(\omega)$ ,  $\tilde{\epsilon}(\omega)$ ,  $\phi_k(\omega)$ , and  $\phi_\epsilon(\omega)$ , which characterize the linearized response of steady-state turbulence to periodic perturbation of the forcing, can be called the *linear response functions*.

We will use periodically forced turbulence as a test case to evaluate the ability of multiple-scale models to predict the dynamics of time-dependent turbulence. It will first be shown that the unsteady predictions of multiple-scale models are significantly better than the predictions of a two-equation model. However, an elementary multiple-scale model based on the heuristic picture of stepwise energy cascade is found to have limitations in predicting the unsteady dissipation rate. A multiple-scale model that includes the possibility of nonlocal interactions is proposed; it is shown that this model can capture some fine features of the unsteady energy dissipation.

The linear response functions were determined in recent work [10] using the EDQNM closure theory, which was shown to compare very well to available low Reynolds number experimental, and DNS data. Comparison with high Reynolds number data for linear response functions would be desirable, but such data is not yet available. Briefly summarizing the major conclusions, the two-equation model is satisfactory both in the *static* limit  $\omega \rightarrow 0$ , in which the phase shifts  $\phi_k, \phi_\epsilon$  vanish, and in the *frozen* limit  $\omega \rightarrow \infty$ , in which  $\tilde{k} \sim \omega^{-1}$  and  $\phi_k \sim \pi/2$ . However, this agreement is trivial; only the results at intermediate frequencies provide a real test of the model. The two-equation model reproduces the function  $\tilde{k}(\omega)$  reasonably well, but the transition from the static limit  $\phi_k \approx 0$  to the frozen limit  $\phi_k \approx \pi/2$  occurs over a frequency range that is much too wide. The amplitude  $\tilde{\epsilon}(\omega)$  is not satisfactory: a range in which  $\tilde{\epsilon} \sim \omega^{-3}$  at high Reynolds numbers is absent. We note that since observations of the modulated dissipation rate are very difficult,

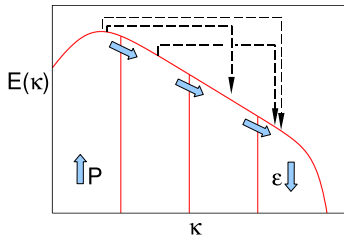


FIG. 1: Schematic view of a discretized energy cascade. The solid arrows indicate the energy fluxes between neighboring wavenumber shells. The dashed lines indicate the nonlocal fluxes between spectrally remote shells. Note that a similar picture can be found in a paper by Lumley [11].

and relevant high Reynolds number data is not yet available, the EDQNM results for this quantity remain theoretical predictions; they are nevertheless supported by arguments [10] based on the well-established role of distant interactions in turbulence. Finally, the two-equation model also makes the incorrect prediction that  $\phi_k = \phi_\epsilon$  regardless of  $\omega$ .

We investigate whether these predictions can be improved using multiple-scale modeling following the ideas of Schiestel [6]. Multiple-scale models can be considered numerical methods for spectral closures, with significant modifications designed to permit reasonable accuracy at a very low order of discretization. Thus, whereas a numerical implementation of a spectral closure would solve for the energy spectrum at perhaps hundreds of discrete wavenumbers  $\kappa_i$ , in Schiestel's formulation, the energy spectrum is divided into a relatively small number of wavenumber shells  $\kappa_{i-1} \leq \kappa \leq \kappa_i$ ; for each shell, equations are written for two scalar descriptors: the fluctuation energy contained in the shell and the net energy flux into it. To enhance the accuracy possible with a relatively small number of shells, Schiestel allowed the partition wavenumbers  $\kappa_i$  to be functions of time. A schematic picture of the resulting discretized energy cascade is given in Figure 1, following Lumley [11].

The starting point for the analytical formulation is the Lin equation governing the energy spectrum  $E(\kappa, t)$ ,

$$\left( \frac{\partial}{\partial t} + \nu \kappa^2 \right) E(\kappa, t) = P(\kappa, t) - \frac{\partial F(\kappa, t)}{\partial \kappa}. \quad (1)$$

In this equation  $\nu$  is the viscosity,  $P(\kappa, t)$  the forcing term, and  $F(\kappa, t)$  is the energy flux across wavenumber  $\kappa$ . Schiestel applied the Kovaznay model [12]

$$F(\kappa, t) = C \kappa^{5/2} E(\kappa, t)^{3/2}, \quad (2)$$

with  $C$  a parameter which determines the Kolmogorov constant. This model represents a stepwise cascade of energy in spectral space from small to large  $\kappa$  and reproduces a  $\kappa^{-5/3}$  inertial range. Figure 1 would correspond to a stepwise cascade if the dashed lines were absent.

To obtain a multiple-scale model, write the equation

for the time derivative of the spectral energy flux  $F(\kappa, t)$ ,

$$\dot{F}(\kappa, t) = \frac{3 F(\kappa, t)}{2 E(\kappa, t)} \dot{E}(\kappa, t). \quad (3)$$

From the viewpoint of Schiestel's analysis, we have assumed that the partition wavenumbers are constant in time: this assumption seems appropriate for this problem, in which the forcing wavenumber is fixed. The production scales are assumed to be confined to low  $\kappa$ , and the dissipation to high  $\kappa$  (a more general description including finite-Reynolds number effects or broad-band forcing will not be attempted here). For  $\kappa$  in the inertial range, (1) becomes

$$\dot{E}(\kappa, t) = - \frac{\partial F(\kappa, t)}{\partial \kappa}. \quad (4)$$

We combine this with (2) and (3) to obtain

$$\dot{F}(\kappa, t) = - \frac{3 F(\kappa, t)}{2 E(\kappa, t)} \frac{\partial F(\kappa, t)}{\partial \kappa}. \quad (5)$$

A discrete model is obtained by splitting the spectral domain into  $n$  shells as illustrated in Figure 1. The energy in shell  $i$  is  $e_i \approx E(\kappa_i) \Delta \kappa_i$ . The spectral flux  $f_i \approx F(\kappa_i)$  and the time derivative is  $\partial F(\kappa_i, t) / \partial \kappa \approx (f_i - f_{i-1}) / \Delta \kappa_i$ , so that we obtain

$$\dot{f}_i = - \frac{3 f_i}{2 e_i} (f_i - f_{i-1}), \quad 1 \leq i \leq n. \quad (6)$$

Integrating (4) over each shell gives the partial energy balance equations

$$\dot{e}_i = -(f_i - f_{i-1}), \quad 1 \leq i \leq n. \quad (7)$$

in which all  $f_i$  and  $e_i$  are functions only of time. The oscillating production term  $\tilde{p}$ , assumed to act at the small wavenumbers, is identified with  $f_0$ , the flux entering shell 1. Furthermore, the high Reynolds numbers case is considered in which we assume that the viscous dissipation takes place at the last wavenumber shell:  $\epsilon = f_n$ . This assumption makes it unnecessary to introduce partial dissipation rates for each shell and corresponding equations of motion. A special feature of the Kovaznay model is that the partition wavenumbers do not appear in the model.

By choosing  $n = 1$ , one obtains a two-equation model; the equation for  $f_1$  becomes the dissipation rate equation  $\dot{e} = (3/2)(\epsilon/k)(P - \epsilon)$ . Note that the two model constants, generally called  $C_{\epsilon 1}$  and  $C_{\epsilon 2}$  in the literature, are equal, which allows the study of statistically stationary isotropic turbulence. Consistency with homogeneous shear flow, or with any problem in which the forcing length scale increases as a power law or exponential in time [13], requires  $C_{\epsilon 1} < C_{\epsilon 2}$ .

Choosing  $n \geq 2$  should improve the predictions by introducing the possibility of spectral imbalance, a necessary requirement if the same model is to be applied to both forced and decaying turbulence [2]; imbalance is

possible because the partial fluxes  $f_i$  with  $1 \leq i \leq n-1$  and the dissipation  $\epsilon = f_n$  are independent.

The unsteady behavior of this model is now assessed as follows. Beginning with a steady state with shell energies  $\bar{e}_i$  such that  $\bar{p} = \bar{f}_i = \bar{\epsilon}$ , the periodic perturbation  $\tilde{p} \cos(\omega t)$  is added to the forcing. Describing the periodic response in terms of complex amplitudes  $\hat{k}(\omega)$  and  $\hat{e}(\omega)$ , so that  $\tilde{k}(\omega) = |\hat{k}(\omega)|$  and  $\tan \phi_k(\omega) = \Im \hat{k}(\omega) / \Re \hat{k}(\omega)$  with the obvious analogs for  $\epsilon$ , the equations for the periodic part of the partial kinetic energies and local fluxes become

$$i\omega \hat{e}_i = -(\hat{f}_i - \hat{f}_{i-1}), \quad i\omega \hat{f}_i = -\frac{3}{2} \frac{\bar{f}_i}{\bar{e}_i} (\hat{f}_i - \hat{f}_{i-1}). \quad (8)$$

The resulting linear system is easily solved analytically for  $\hat{e}_i(\omega)$  and  $\hat{f}_i(\omega)$  in terms of the periodic forcing perturbation  $\tilde{p}$  and the parameters  $\bar{e}_i$  and  $\bar{f}_i$ .

Figure 2 compares the results for the amplitude  $\tilde{k}(\omega)$  and phase shift  $\phi_k(\omega)$  for models with  $n = 1$  to  $n = 7$  wavenumber shells. Also shown are results obtained in EDQNM computations [10] at Reynolds number  $R_\lambda = 1000$ , with  $R_\lambda \approx 15R_L^{1/2}$  and  $R_L = (2\bar{k}/3)^{1/2} \bar{L}/\nu$ . It has been shown [10] that at low  $\omega$ ,  $\tilde{k}(\omega)$ , should tend to a plateau and that at large  $\omega$ ,  $\tilde{k}(\omega)$  follows a power-law proportional to  $\omega^{-1}$ . Confirming the conclusion of Bos *et al.*[10],  $\tilde{k}(\omega)$  is in reasonable agreement with EDQNM even for the two-equation model  $n = 1$ , although this agreement improves significantly as the number of wavenumber partitions  $n$  increases.

The error in the two-equation model prediction of  $\tilde{k}(\omega)$  is a too gradual transition from the plateau to the  $\omega^{-1}$  region. This defect appears more prominently in the phase  $\phi_k(\omega)$ : although all models give the correct static and frozen limits, the two-equation model transitions much too gradually, and only the models with  $n \geq 2$  are in close agreement with EDQNM. The relatively rapid transition in the energy phase shift therefore appears as a typical multiple-scale effect: evidently, in this problem, the small scales are not simply ‘slaved’ to the large scales through a constant dissipation rate as is assumed in a two-equation model; instead, they are dynamically independent and have a strong effect on what is apparently a purely large-scale property.

It has also been demonstrated[10] that the response function  $\tilde{\epsilon}(\omega)$  follows at high  $\omega$  a power-law proportional to  $\omega^{-3}$  up to the Kolmogorov frequency  $\omega_\eta \sim \bar{\epsilon}/\nu$ . For  $\omega > \omega_\eta$ ,  $\tilde{\epsilon}(\omega)$  becomes proportional to  $\omega^{-1}$ . These results are shown for comparison in the graph on the left side of Figure 3 (the phase shift  $\phi_\epsilon$  proves difficult to compute with any confidence because of the extremely small amplitudes involved, therefore comparisons are omitted).

The agreement of  $\tilde{\epsilon}(\omega)$  given by the multiple-scale model Eq. (8) with the EDQNM results is very good down to values  $\tilde{\epsilon}/\bar{p} = 10^{-3}$  for  $n > 3$  (note that  $\tilde{k}(\omega)$  and  $\tilde{\epsilon}(\omega)$  are proportional to  $\tilde{p}$ , and  $\tilde{p}$  is chosen unity without loss of generality). However for smaller values of  $\tilde{\epsilon}/\bar{p}$ , the discrete model starts to diverge from the EDQNM results, especially for large  $n$ . It is very easily shown that

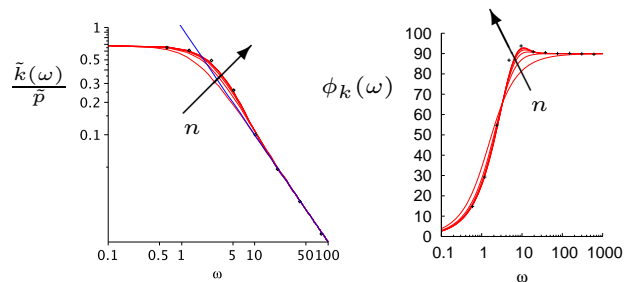


FIG. 2: Linear response functions  $\tilde{k}(\omega)$  (left) and  $\phi_k(\omega)$  (right) for the multiple-scale model based on the Kovaznay spectral closure (6). The 7 curves in each graph correspond to models with  $n = 1, 2, \dots, 7$  spectral shells and  $n$  increases in the direction of the arrow. The theoretical amplitude prediction  $\omega^{-1}$  is indicated by a straight line. Also shown are the results of EDQNM simulations (symbols). The frequency  $\omega$  is normalized by the large scale frequency  $\bar{\epsilon}/\bar{k}$ .

for this model, the leading order contributions at high  $\omega$  are proportional to  $\omega^{-n}$ : indeed, recursive solution of the equations for  $\hat{f}_i$  in (8) show that  $\hat{f}_i \sim \omega^{-i}\tilde{p}$ . Thus, only if  $n = 3$  can we obtain  $\tilde{\epsilon}(\omega) \sim \omega^{-3}$ , but this is the result of a coincidence, which disappears if the number of partition wavenumbers is increased. This difficulty reflects a limitation of the multiple-scale model: Eq. (5) implies a linear first-order partial differential equation for  $\hat{F}$  in which disturbances in  $F$  propagate along characteristics; this property is probably significantly compromised by a finite dimensional approximate model.

It has been shown[10] that nonlocal interactions are responsible for the  $\omega^{-3}$  range. Nonlocal interactions are represented in Figure 1 by dashed lines. Such interactions do not occur in the model Eqs. (6) and (7), because quantities in shell  $i$  depend only on its nearest neighbor, shell  $i-1$ . The absence of nonlocal interactions will be even more significant in problems in which the role of nonlocality is greater, as in the Batchelor regime of the passive scalar [14] and in MHD [15].

To address this problem, a new multiple-scale model will now be derived including the effect of nonlocal interactions. We start from a simple spectral model containing nonlocal interactions, due to Ellison [12],

$$F(\kappa, t) = C \left( \int_0^\kappa \kappa'^2 E(\kappa', t) d\kappa' \right)^{1/2} \kappa E(\kappa, t). \quad (9)$$

Applying the same procedure as to the Kovaznay model, the partial energy balance Eq. (7) is unchanged, but Eq. (6) is replaced by

$$\dot{f}_i = -\frac{f_i}{e_i} (f_i - f_{i-1}) - \frac{f_i}{2} \frac{\sum_{p=1}^i \kappa_p^2 (f_p - f_{p-1})}{\sum_{p=1}^i \kappa_p^2 e_p}. \quad (10)$$

This expression contains the wavenumbers  $\kappa_i$  because nonlocal interactions, which depend on the spacing between the wave-number partitions, have been retained. The specification of the  $\kappa_i$  becomes part of the model:

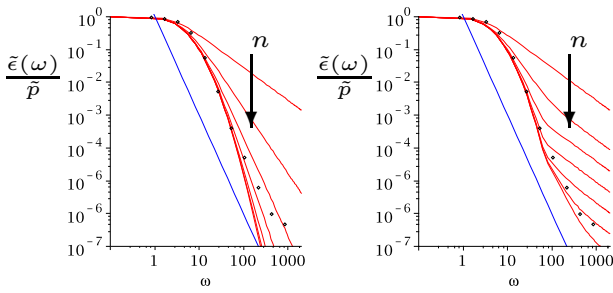


FIG. 3: Frequency response function  $\tilde{\epsilon}(\omega)$  for the model based on the Kovaznay closure (8) (left) and for the model based on the Ellison closure (11) (right). The 7 curves in each graph correspond to  $n = 1, 2, \dots, 7$  and  $n$  increases in the direction of the arrow. The theoretical prediction  $\omega^{-3}$  is indicated by the straight lines. Also shown are the results of EDQNM simulations (symbols).

we will use a logarithmic discretization with  $\kappa_i = \kappa_1 r^{i-1}$  in which  $r$  is a model parameter which determines the logarithmic gridsize. Using this discretization, the ratio  $\kappa_n/\kappa_1 = r^{n-1}$ , so that a large range of scales can be considered by increasing  $r$ . Note that if a linear discretization is used,  $\kappa_n/\kappa_1 = (n\Delta\kappa/1\Delta\kappa) = n$  so that the number of partitions for high Reynolds numbers becomes prohibitively large. Using the logarithmic discretization, the model for periodic forcing becomes

$$\hat{f}_i = -\frac{\tilde{f}_i}{\tilde{e}_i}(\hat{f}_i - \hat{f}_{i-1}) - \frac{\tilde{f}_i \sum_{p=1}^i r^{2(p-1)}(\hat{f}_p - \hat{f}_{p-1})}{2 \sum_{p=1}^i r^{2(p-1)}\tilde{e}_p}, \quad (11)$$

with the same partial energy equations as in Eq. (8). Again, when  $n = 1$  the model reduces to a two-equation model. For  $n > 1$  the model differs from the previous model through the interaction term which couples wavenumber shell  $i$  with all wavenumber shells  $p = 1, \dots, i$ . The response functions depend on both  $n$  and  $r$ , which

will be chosen through a compromise between computational cost and precision.

The results for  $\tilde{\epsilon}(\omega)$  obtained from Eq. (11) with  $r = 3$  and  $1 \leq n \leq 7$  wavenumber partitions are shown in the graph on the right side of Figure 3. In the same figure, EDQNM results [10] at  $R_\lambda = 1000$  are shown. The agreement with EDQNM is very good down to values  $\tilde{\epsilon}/\tilde{p} = 10^{-3}$  for  $3 < n < 7$ , and for  $n = 7$ , agreement is good down to  $\tilde{\epsilon}/\tilde{p} = 10^{-6}$ . We conclude that the model including nonlocal interactions Eq. (11) makes better predictions of  $\tilde{\epsilon}$  than the model Eq. (8), in which nonlocal interactions are absent. The predictions of Eq. (11) (not shown) for  $\tilde{k}(\omega)$  and  $\phi_k(\omega)$  very nearly coincide with the results obtained using Eq. (8).

To conclude, we have found that in the problem of periodically forced turbulence, a two-equation model only gives satisfactory predictions for  $\tilde{k}(\omega)$  and  $\phi_k(\omega)$  at asymptotically high and low frequencies. The predictions at intermediate frequencies are improved by using a multiple-scale model based on the heuristic picture of stepwise energy cascade, the Kovaznay model. In particular, this model correctly predicts the rapid jump of the phase shift  $\phi_k(\omega)$  between the static and frozen limits. The multiple-scale model based on the Ellison closure includes nonlocal effects, and leads to better agreement with EDQNM, including the high Reynolds number  $\omega^{-3}$  scaling range [10]. Both models give practically indistinguishable results for the amplitude and phase of the oscillating kinetic energy, which is not strongly influenced by nonlocal interactions. Our approach suggests how one might construct reduced order models for phenomena dominated by significant nonlocal interactions, like the Batchelor range of the passive scalar and some cases of MHD.

We would like to acknowledge the interesting and thoughtful comments of the referees, which led to significant modifications of the paper.

- 
- [1] M. Oberlack. Similarity in non-rotating and rotating turbulent pipe flows. *J. Fluid Mech.*, 379:1, 1999.
  - [2] W.J.T. Bos, L. Shao, and J.-P. Bertoglio. Spectral imbalance and the normalized dissipation rate of turbulence. *Phys. Fluids*, 19(045101), 2007.
  - [3] R. Rubinstein, T. Clark, D. Livescu, and L. Luo. Time-dependent isotropic turbulence. *J. Turbul.*, 5:011, 2004.
  - [4] H. Tennekes and J.L. Lumley. *A first course in turbulence*. MIT Press, Cambridge MA, 1972.
  - [5] H. Touil, S. Parpais, and J.P. Bertoglio. A spectral closure applied to anisotropic inhomogeneous turbulence. in *Advances in Turbulence 8 (Dopazo ed.)*, Barcelona 2000.
  - [6] R. Schiestel. Multiple-time-scale modeling of turbulent flows in one-point closures. *Phys. Fluids*, 30:722, 1987.
  - [7] D. Lohse. Periodically kicked turbulence. *Phys. Rev. E*, 62:4946, 2000.
  - [8] O. Cadot and J. H. Titon and D. Bonn. Observation of resonances in modulated turbulence *J. Fluid Mech.*, 485:161, 2003.
  - [9] A.K. Kuczaj, B.J. Geurts, D. Lohse, and W. van de Water. Turbulence modification by periodically modulated scale-dependent forcing *Comput. Fluids*, 37:816, 2008.
  - [10] W.J.T. Bos, T.T. Clark, and R. Rubinstein. Small scale response and modeling of periodically forced turbulence. *Phys. Fluids*, 19, 2007.
  - [11] J.L. Lumley. Some comments on turbulence. *Phys. Fluids*, 4:206, 1992.
  - [12] A. S. Monin and A. M. Yaglom. *Statistical Fluid Mechanics*. MIT Press, Cambridge MA, 1975.
  - [13] R. Rubinstein and T. Clark, Self-similar turbulence evolution and the dissipation rate transport equation. *Phys. Fluids*, 17:095104, 2005.
  - [14] G.K. Batchelor. Small-scale variation of convected quantities in turbulent fluid. *J. Fluid Mech.*, 5:113, 1959.
  - [15] A. Pouquet, U. Frisch, and J. Léorat. Strong MHD helical turbulence and nonlinear dynamo effect. *J. Fluid Mech.*,

77:321, 1976.